AORTIC DISEASE ASSESSMENT BY MULTIDETECTOR CT AORTOGRAM

Ummara Siddique Umer, Syed Ghaus, Shahjehan Alam, Seema Gul

Department of Radiology, Rehman Medical Institute, Peshawar, Pakistan.

PJR April - June 2016; 26(2): 99-109

ABSTRACT

PURPOSE: To evaluate the reliability of 128 slice Multidetector computed tomographic (MDCT) angiography in differentiating different types of aortic diseases and for preoperative aortic morphologic assessment. **MATERIALS AND METHODS:** 116 patients underwent pre-operative CT aortography on 128 slice Toshiba CT scanner in the Radiology department of Rehman Medical Institute Peshawar, over a period of one year. With a breath-hold of 15 to 20 seconds and 1 or 2 mL/kg (80 to 150 mL) of nonionic contrast by power injector at 3 to 5 mL/s, axial images from above the arch to the femoral arteries were obtained and reconstructed at 0.5 mm intervals. ECG gated study was done in those cases having suspicion of aortic root involvement on echocardiography. Pre-contrast scans were obtained in patients with symptoms of acute aortic syndrome. Axial images were reformatted to yield 3-dimensional (3D) images. Images were reviewed on 5.1 vitrea workstation for type and location of pathologic lesions. Imaging findings were compared with surgical findings. **RESULTS:** The types of aortic abnormalities present in the patients included: Coarctation (25%), thoracic aortic aneurysms (22%), Dissections (19%), Thoraco-abdominal diffuse aortic ectasia (2%), Pseudo aneurysms/ Mycotic aneurysms (2%), PDA aneurysms (3%), Interrupted aorta (2%), Right sided aortic arch (2%), Kommerell diverticulum (2%), aortitis (2%), midaortic syndrome (1%) and leriche syndrome (1%). Atherosclerosis was seen in multiple Aortograms. Different anatomical congenital variations were seen; commonest was common origin of right brachiocephalic and left common carotid arteries. Aberrant right subclavian artery was seen in 2 of the cases. Right sided aortic arch was also seen in 2 cases. The accuracy of diagnosis by CT was 100%. **CONCLUSION:** MDCT with the use of multiplanar reconstruction enables highly accurate differentiation among diseases of the aorta. MDCT angiography with multiplanar and three-dimensional techniques should be the method of choice for preoperative morphologic assessment of aortic diseases in adult patients.

Key words: Aortic diseases, aortic aneurysm, aortic dissection, multidetector CT.

Introduction

State-of-the-art multidetector computed tomographic (MDCT) technology has replaced invasive angiography for evaluation of patients suspected to have aortic disease. Although most aortic disease is associated with atherosclerosis (i.e., aneurysms and dissection), the spectrum of aortic disease is vast and includes various congenital and acquired entities. Radiologists should be familiar with uncommon aortic diseases, which are divided into those that are congenital in origin and acquired disorders, and with their findings at multidetector CT.[1] Imaging information that is important to surgeons includes the diagnosis, location of lesion and extent of disease. The purpose of our study was to assess the accuracy of MDCT in differentiating among different aortic diseases.

Brief Anatomy of Aorta:

Aorta has two major components; Thoracic aorta

Correspondence : Dr. Ummara Siddique
Department of Radiology,
Rehman Medical Institute,
Peshawar, Pakistan.
Phone: +92 321 9141788
Email: ummara_81@hotmail.com

Submitted 25 October 2015, Accepted 2 December 2015

and abdominal aorta. The thoracic aorta can be divided into several segments, namely, the root, ascending aorta, arch, and descending aorta. The root has three components: the annulus, the sinuses of Valsalva and the sinotubular junction. The coronary arteries originate from the sinuses adjacent to the sinotubular junction. The ascending aorta extends from the sinotubular junction to the origin of brachiocephalic artery. The arch extends from the brachiocephalic artery origin to the left subclavian artery origin. Its most distal aspect, which is often slightly narrowed, is termed the "aortic isthmus." The descending thoracic aorta extends from the ligamentum arteriosum to the level of the diaphragmatic hiatus.[2] The most proximal portion of the descending thoracic aorta appears slightly dilated and is called the aortic spindle.[3] Three great arterial branches arise sequentially from the aortic arch. The innominate artery is the first and typically the largest branch and is usually seen more caudally than the other branches on transverse CT images. It gives rise to the right subclavian and right common carotid arteries. The left common carotid artery arises next at a more cephalad level and has the smallest diameter of the three major arterial branches. The left subclavian artery is the third branch and arises from the posterior superior portion of the aortic arch.This normal branching pattern is seen in about 70% of individuals.[4] The most common variation is a combined origin of the innominate and left common carotid arteries, which is seen in about 20 - 30% of individuals. The abdominal aorta extends from the diaphragm to the level of the fourth lumbar vertebra, where it bifurcates into the right and left common iliac arteries. The abdominal aorta gives rise to important single and paired branches. The single branche s arise anteriorly and supply the anterior abdomen, whereas the paired branches arise laterally and supply the posterior abdomen. The single branches include the celiac trunk, which arises close to the diaphragmatic crus; the superior mesenteric artery, which arises immediately caudally; and the inferior mesenteric artery, which arises just above the aortic bifurcation.[5] The unpaired middle sacral artery arises from the posterior terminal portion of the abdominal aorta. The paired abdominal aorta branches are, from cephalad to caudal, the inferior phrenic arteries, suprarenal and renal arteries, gonadal arteries, and several paired lumbar arteries. Variations of the abdominal aorta branches are common and knowledge of these variations facilitates their accurate identification and protection during surgery.[6]

Aortic measurements:

Accurate measurement of the aorta is vital in follow-up of aortic diseases especially in thoracic aortic aneurysms and determining suitability for surgical or endovascular repair. Aortic measurements are made in true short axis projection acquired from double oblique views, from one blood-wall boundary to the other. With CT, ECG gating is essential for accurate measurement, particularly in the ascending aorta (Fig. 1). Based on normative data collected from a large sample population in a study, the intraluminal diameter of the ascending aorta (mean ± 2 SDs) in young adults (20 - 40 years) has been shown to vary between 35.6 and 37.8 mm for women and men, respectively, with a statistically significant linear association with age, sex, descending aortic diameter, and pulmonary artery diameter.[7] The aorta tapers distally, with the normal descending aorta always smaller in caliber than the ascending aorta in healthy individuals. The proximal descending aorta is considered abnormal when it exceeds 2.63 cm, and the distal descending aorta is considered abnormal when it exceeds 2.43 cm in diameter.[8,9] The normal abdominal aorta usually does not exceed 2 cm in diameter in healthy individuals.[10] Table (Tab. 1) provides practical values of the generally accepted maximal normal

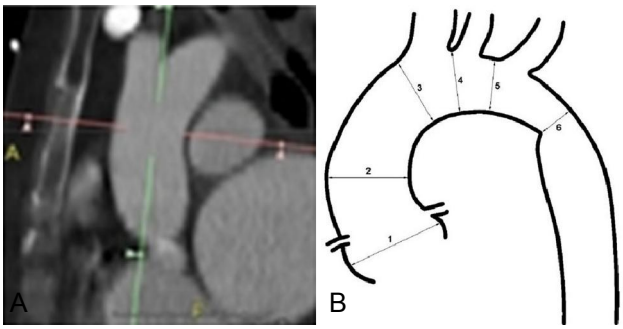

Figure 1: Measurement of aortic size by CT scan. **(a)** Double oblique short axis image of mid ascending aorta acquired from orthogonal coronal and sagittal images at the level of mid ascending aorta. **(b)** The thoracic aortic diameters were measured at different levels as follows: 1, aortic valve sinus; 2, proximal ascending aorta at the level of the right pulmonary artery; 3, proximal to the innominate artery; 4, proximal transverse aortic arch; 5, distal transverse aortic arch; and 6, aortic isthmus.

diameters of the ascending, descending, and abdominal aorta. In explaining the diameter differe-nces, one should consider the nature of the changes in the diameter of an aging aorta, which grows roughly 1 mm per year.[11]

Segment	Size
Ascending	4
Descending thoracic	3
Abdominal	2

Table 1: Maximal Normal Aortic Diameter

Materials and Methods

116 patients underwent CT aortography on 128 slice Toshiba CT scanner in the Radiology department of Rehman Medical Institute Peshawar, over a period of one year. With a breath-hold of 15 to 20 seconds and 1 or 2 mL/kg (80 to 150 mL) of nonionic contrast by power injector at 3 to 5 mL/s, axial images from above the arch to the femoral arteries were obtained and reconstructed at 0.5 mm interval. Pre-contrast scans were obtained in patients with symptoms of acute aortic syndrome. Axial images were reformatted to yield 2-dimensional (2D) images and 3-dimensional (3D) images. Images were reviewed on 5.1 vitrea workstation for type and location of pathologic lesions. Imaging findings were compared with surgical findings.

Technique:

In evaluation of the aorta, multidetector CT angiography protocol was primarily non-gated. However, in some specific situations, electrocardiographically (ECG) - gated studies were performed e.g. when the concern was to assess aortic root involvement, visualization of the coronary arteries and for better delineation of the ventricular and atrial septa and cardiac chambers. To decrease the effective radiation dose, different dose modulation techniques were used. In particular, 100 kV was used in all pediatric patients and in selected adults (body weight less than 90kg). In this article, we reviewed cases with congenital aortic anomalies, common and some uncommon encountered acquired aortic diseases and role of MDCT in acute aortic syndrome.

Results

The types of aortic abnormalities present in the patients included: Coarctation (25%), thoracic aortic aneurysms (22%), Dissections (19%), Thoraco-abdominal diffuse aortic ectasia (2%), Pseudo aneurysms/ Mycotic aneurysms (2%), PDA aneurysms (3%), Interrupted aorta (2%), Right sided aortic arch (2%), Kommerells diverticulum (2%) and aortitis (2%), midaortic syndrome (1%) and leriche syndrome (1%). Atherosclerosis was seen in multiple Aortograms. Different anatomical congenital variations were seen; commonest was common origin of right brachiocephalic and left common carotid arteries. Aberrant subclavian artery was seen in 2 of the cases. Right sided aortic arch was also seen in 2 cases. The accuracy of diagnosis by CT was 100%.

Discussion

Aortic Dilatation:

The normal aortic annulus measures 26.3 mm ± 2.8 mm in the coronal plane and 23.5 ± 2.7 mm in the sagittal plane with no significant change between systole and diastole, according to a study published in 2008 by Tops et al.[12] The normal ascending aorta measures 3.6 cm in females and 3.8 cm in males.[13] The proximal descending aorta is considered enlarged when it exceeds 2.6 cm and the distal descending aorta is considered enlarged when it exceeds 2.4 cm. However, for simplicity, the ascending aorta is considered to be enlarged when it is larger than 4 cm and the descending aorta when it is larger than 3 cm. An aneurysm is diagnosed when the ascending aorta is larger than 5 cm and the descending aorta is larger than 4 cm.[13] High risk for aortic rupture or dissection is when aortic diameter exceeds 6 cm for descending thoracic aorta and 7cm for abdominal aorta. Aortic root dilatation is associated with risk factors of coronary artery disease and predicts cardiac failure, stroke, and all causes of cardiovascular mortality.[14]

In our study, 22 patients had aortic root dilatation or ectasia and two patients had diffuse ectasia of thoracoabdominal aorta.

Annuloaortic Ectasia:

Annuloaorticectasia is symmetric dilation of the aortic root and ascending aorta with effacement of the sinotubular junction. The ascending aorta has a pear shaped appearance and the arch is of normal caliber. It most commonly occurs with Marfan syndrome. Ascending aortic aneurysm is also seen in syphilis, bicuspid aortic valve, aortitis, and postoperative patients. (Fig. 2d) shows 3D reformatted image of CT Aortogram in a young patient having pear shaped dilated aortic root and ascending aorta with effacement of the sinotubular junction consistent with annuloaorticectasia.

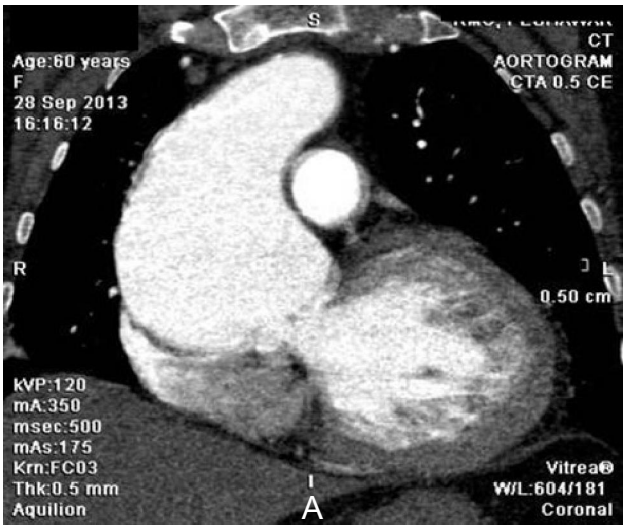

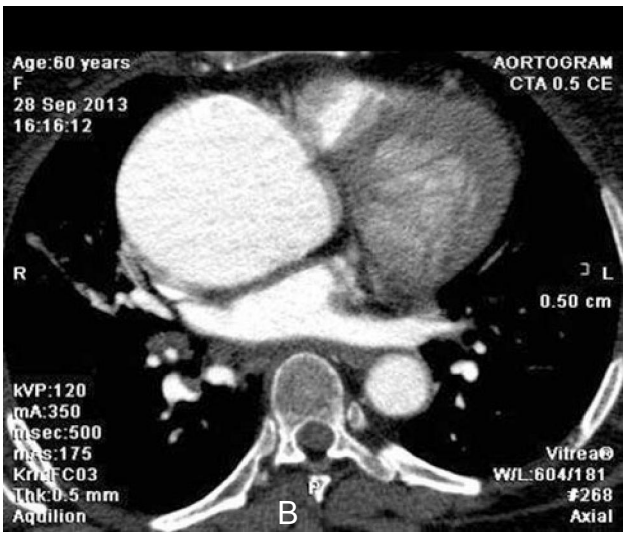

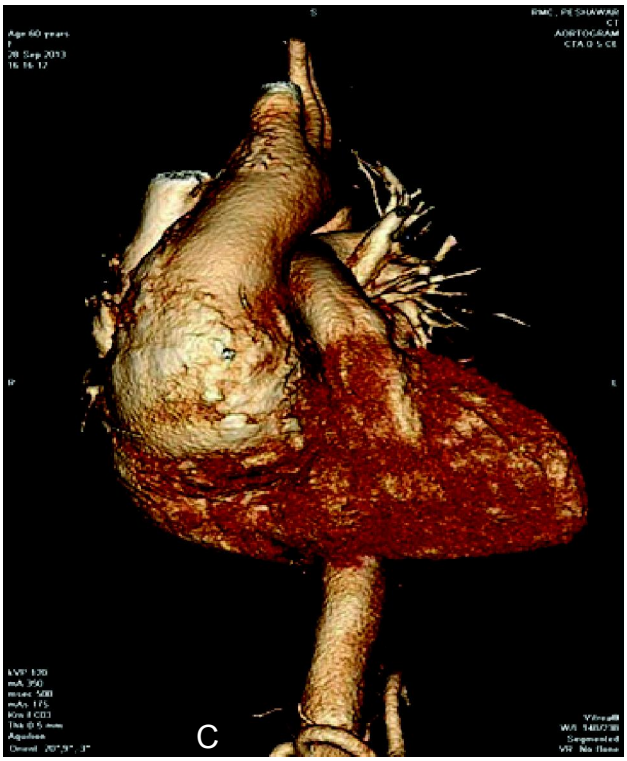

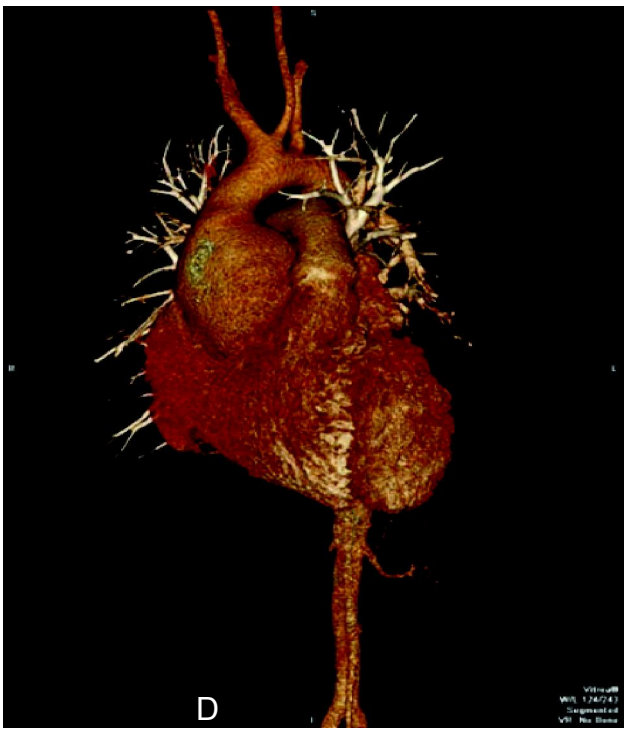

Figure 2 (a,b,c&d): (a,b&c) Curved coronal, axial reformatand 3D voulme rendered images showing large ascending aortic aneurysm involving the sinus of valsalva and ascending aorta. **(d)** Volume rendered 3D reformatted image of CT Aortogram in a young patient having pear shaped dilated aortic root and ascending aorta with effacement of the sinotubular junction consistent with Annuloaortic ectasia.

Aneurysm:

An aneurysm is defined as permanent localized dilation of the aorta, either 50% or 2 standard deviations larger than normal expected diameter for that aortic segment.[15] Aneurysms are most common in the ascending segment (60%), followed by descending segment (40%) and arch (10%). Both thoracic and abdominal segments are affected in 10% of patients with aortic aneurysm.[16] Aneurysms are classified as either fusiform or saccular. A fusiform aneurysm has symmetrical dilation involving the entire circumference of the aortic wall, while a saccular aneurysm is more localized with outpouching of one portion of the aortic wall. All the three mural layers are involved in true aneurysm and not involved with pseudoaneurysms (false aneurysms), which are often associated with intimal and, occasionally, medial disruption. Pseudoaneurysms are usually saccular and are most commonly the result of trauma, infection, instrumentation, or penetrating atherosclerotic ulcers. When a saccular aneurysm has a wide neck, there is a high possibility that it is a mycotic aneurysm (Fig. 3). In our study, ascending aortic aneurysms were in seen in 22 cases. These patients had true fusiform aneurysms (Fig. 2a,b&c). One patient had bicuspid aortic valve.

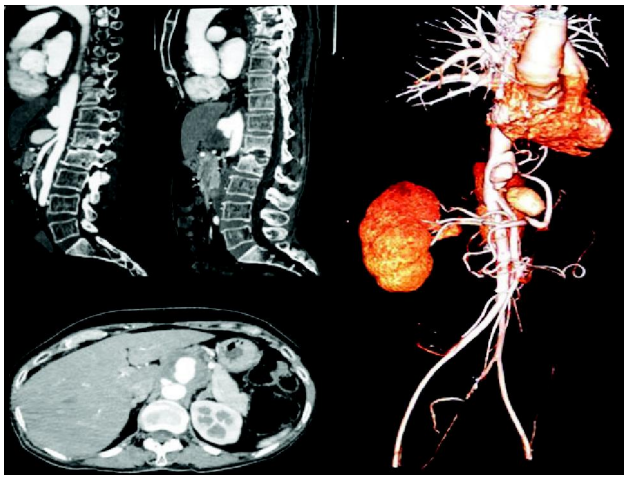

Figure 3: 50 years old female with saccular mycotic aneurysm of aorta and celiac artery. Sagittal images show multilevel spondylodiscitis consistent with caries spine. The aneurysm has a wide neck and partly thrombosed lumen.

Thoracoabdominal aneurysms has been classified based on location using the modified Crawford classification system: type I from level of left subclavian origin to above the renal arteries; type II from the left subclavian artery origin to below the renal arteries; type III from the level of sixth intercostal space to below renal arteries (Fig. 4); type IV from level of 12th intercostal space to below the renal arteries (total abdominal aortic aneurysm); and type V from level of sixth intercostal space to above the renal arteries.[16]

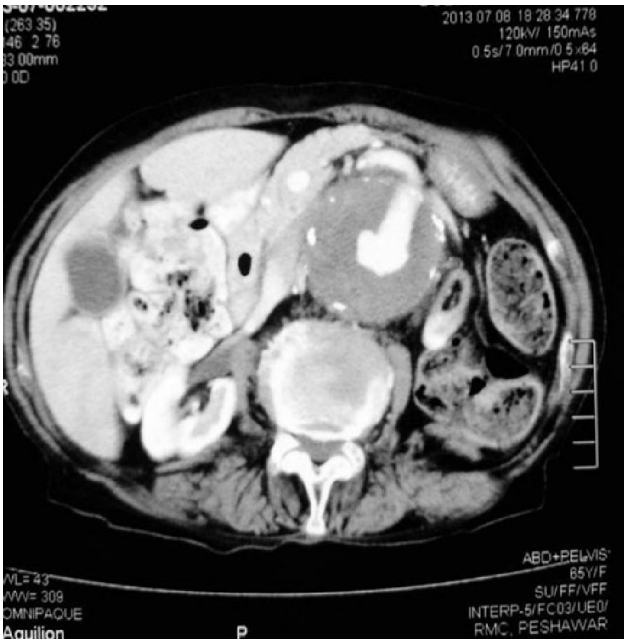

Figure 4: Thrombosed aneurysm of abdominal aortain a 65 years old female. It is involving the origin of Superior mesenteric artery.

Traumatic pseudoaneurysm most commonly occurs at the isthmus (90%) and less commonly in the ascending aorta or descending aorta near the diaphragmatic hiatus.[15]

Mycotic Aneurysm:

In our study, two patients had mycotic aneurysms. One had multilevel caries spine with a large mycotic aneurysm of abdominal aorta involving origin of celiac trunk (Fig. 3). Other patient had a saccular aneurysm of proximal descending thoracic aorta. Mycotic aneurysms are more common in the ascending aorta because of their proximity to regions affected by endocarditis. Mycotic aneurysms can be multiple and are usually saccular with a wide neck.[15] Mycotic aneurysm can be caused by nonsyphilitic organisms such as nonhemolytic Streptococcus, Staphylococcus, S. pneumoniae, Gonococcus, and Salmonella.

Dissection: Aortic dissection is characterized by a tear in the tunica intima of the aorta, with resultant leak of blood into the tunica media and formation of a false lumen. Dissection is the most common cause of acute aortic syndrome and is usually the result of systemic hypertension. Aortic dissection is defined as acute when signs and symptoms persist for fewer than two weeks and chronic if they persist more than two weeks. The Stanford classification is used to describe aortic dissection as it dictates treatment. Type A dissections involve the ascending aorta (Fig. 7) and type B dissections do not involve the ascending aorta (Fig. 5). The older DeBakey classification is as follows: type I-tear originates in ascending aorta and propagates to at least arch and often beyond it; type II-tear originates in and is confined to ascending aorta; and type III-tear originates in proximal descending aorta and extends distally to descending thoracic or thoracoabdominal aorta.[17]

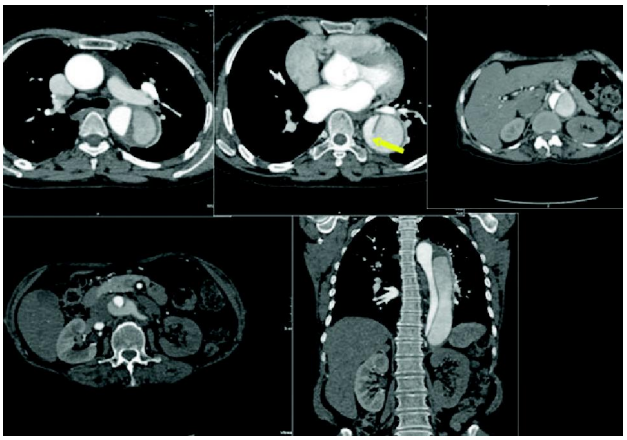

Figure 5: Stanford B dissection.Dissection flap in descending aorta with both true and false lumens. Arrow shows site of flap tear. Celiac trunk has origin from true lumen. Left renal artery is being supplied by false lumen with resultant hypoperfused left kidney.

On unenhanced CT, endoluminal displacement of intimal calcification may be apparent with aortic dissection. Following contrast administration, CT shows an intimal flap separating true from false lumen (Fig. 5). The true lumen maintains direct continuity with the undissected proximal normal aorta and is usually smaller than the false lumen. The false lumen can also be identified by the presence of Cobweb sign (Fig. 6), which describes low attenuation linear foci resulting from residua of incompletely sheared media and the beak sign, which describes

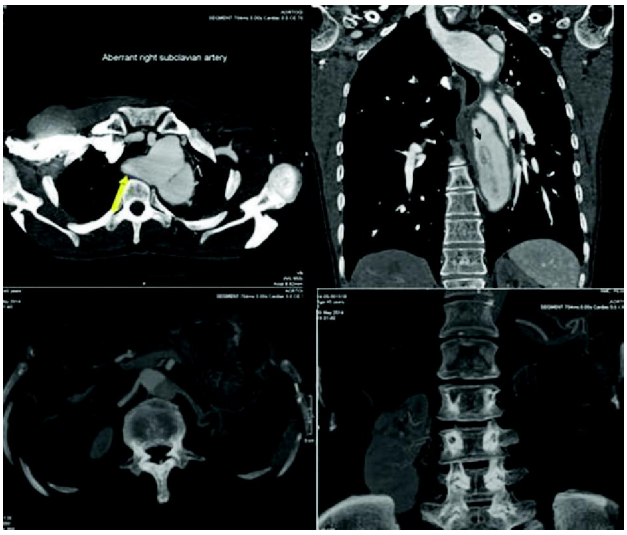

Figure 6: Stanford B dissection in a 45 years old female. Cobweb sign seen in the false lumen (small arrow). There is aberrant right subclavian artery with kommerell's diverticulum (long arrow). Lower images show left kidney being supplied by the false lumen with resultant hypoperfusion of left kidney.

a wedge of hematoma at the leading edge of the false lumen propagation. With triple barreled dissections, three lumens are present, and either reflects two coexistent dissections on either side of the true lumen or a new third lumen within the wall of false lumen. These most commonly occur with Marfan syndrome. In intimointimal intussception, a circumferential dissection invaginates into itself, with one lumen wrapped around the other, most commonly occurring in the arch.

Thrombus within an aneurysm can mimic aortic dissection. Thrombus has a constant circumferential relationship with the aorta and has irregular borders, and intimal calcification is seen peripheral to the thrombus; however, a dissection has a spiral configuration, smooth inner border, and endoluminal displacement of the intimal calcification by the false lumen.[17,18]

Complications of aortic dissection include aortic rupture, hemothorax, mediastinal hematoma, hemopericardium, aortic branch vessel obstruction and end-organ ischemia. Rupture manifests on CT as irregular aortic wall with active contrast extravasation with high attenuation collectionin the pericardium, left extrapleural space or mediastinum. Rarely, mediastinal blood can seep through the adventitial space between the aorta and pulmonary artery and eventually dissect the pulmonary artery. Blood seeping

from the posterior wall of the aorta can also reach the lung tracking along the bronchovascular sheaths. End-organ ischemia results from extension of the dissection flap into the artery supplying the organ or thrombosis of a true or false lumen that supplies the visceral artery in question (Fig. 6). Arterial obstruction can be either dynamic with prolapse of the intimal flap covering the false lumen or static resulting from compression of the artery by the expanding false lumen or adjacent hematoma. A small true lumen with concavity to the false lumen indicates low pressure and possibility of ischemia. Static obstruction is relieved by placing a stent, but dynamic obstruction requires fenestration to relieve pressure in false lumen.[17]

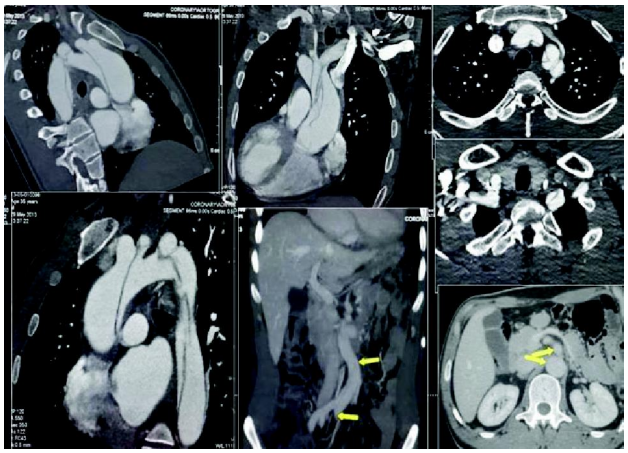

Figure 7: 35 years old male with acute chest pain. Curved MPR images reveal STANFORD A dissection. Arrows on axial image showing involvement of superior mesenteric artery.

Type A dissections require prompt surgical treatment because of the high risk of rupture and cardiac tamponade. Uncomplicated type B dissections are usually treated medically and require serial followup with CT or MRI. Type B dissections with complications require endovascular or surgical repair.

Intramural hematoma:

Intramural hematoma (IMH) is characterized by spontaneous hemorrhage into the tunica media of the aorta, most commonly the result of rupture of the vasa vasorum and less commonly the result of penetrating atherosclerotic ulcer or trauma. It is only visible on non-contrast CT scan. So, patients with symptoms of acute aortic syndrome must have a non-contrast CT before CT aortography.

Aortitis: Aortitis (vasculitis) is characterized by inflam-mation of aortic wall with reactive damage to mural structures (Fig. 8). Takayasu arteritis and giant cell arteritis are the most common vasculitides to affect the aorta. CT shows thickening of the vessel wall and mural contrast enhancement in early stages; stenoses, occlusion, and aneurysms characterize the later stages.[19] Thickened aortic cusps and pericardial effusion or thickening may also be present.[20]

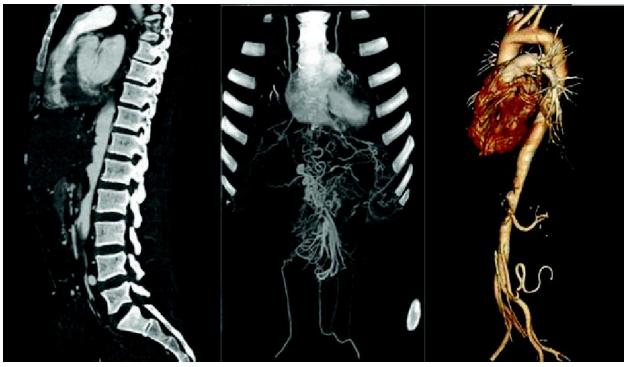

Figure 8: 27 years old male presented with long standing intermittent episodic abdominal pain. CT Aortogram sagittal, coronal and 3D surface rendered images showing irregular thickening of anterior wall of upper abdominal aorta, consistent with aortitis. Numerous collaterals noted.

Traumatic Aortic Injury:

CT is the most commonly used examination for evaluation of the aorta in the setting of trauma and is highly sensitive and specific. Direct CT findings of acute aortic injury include deformity of the aortic contour, intimal flap, intraluminal debris, pseudo-aneurysm, and intramural hematoma.[21] Pseudoaneurysm and intramural hematoma are the most common findings. We did not encounter any post traumatic aortic injury in any of our patients.

Atherosclerosis:

Patchy areas of calcified and noncalcified mural and intimal plaques were seen in most of the aging aortas. On CT Aortogram, irregularity of plaque surface is concerning for ulcer formation. CT is useful in assessing involvement of main branches at their origin. Severity of disease usually ranges from mild to severe. Atherosclerotic disease can also manifest as atheromas, protruding atheromas, atherosclerotic debris and plaque. The mobile components to these plaques have been called mobile debris, mobile pla-

que and superimposed thrombi. These mobile lesions are most often thrombi. Clinical data show that the plaques with high risk for embolization are those that are ≥ 4 mm thick. The term complex plaque has been used in the literature to refer to those plaques that are severe (≥ 4 mm thick), contain mobile elements (most often thrombi), or both.[22] In several case reports, there is direct evidence that severe aortic plaque does in fact cause embolization. CT scanning is probably the current technique of choice for evaluating vascular calcification. As is the case with MRI, most cardiologists do not routinely refer patients with stroke for CT scanning to image aortic plaques.[22]

Leriche Syndrome:

Aorto-iliac occlusive disease is most frequently a chronic condition related to the deposition of atherosclerotic plaque at the level of the aortic bifurcation[23] (Fig. 9). A few notable collateral pathways require reporting by the radiologist because they can change surgical management. The Winslow pathway must be mentioned to avoid iatrogenic damage due to the failure to recognize this artery as a collateral source of blood supply to the lower extremities.[23]

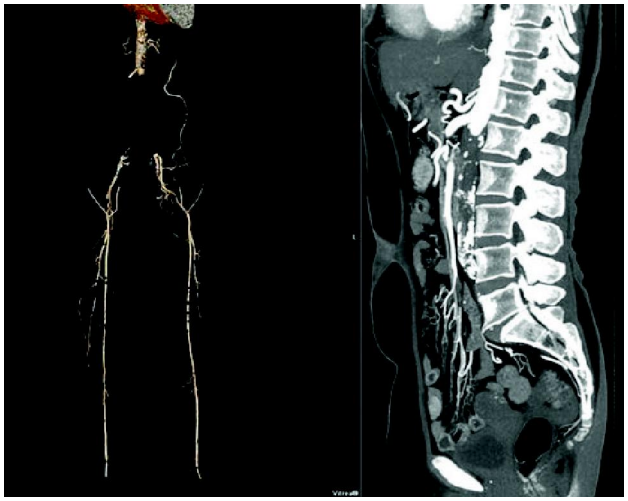

Figure 9: Leriche disease; severe atherosclerotic disease occluding the abdominal aorta and aortic bifurcation. Multilevel focal stenosis seen in both lower limb arteries evident on 3D volume rendered image.

Arteriovenous Fistula (AVF):

Ateriovenous fistula is an abnormal communication between aorta and vein. In our study, one CT aortogram showed a large AVF between aorta and right common iliac vein (Fig. 10).

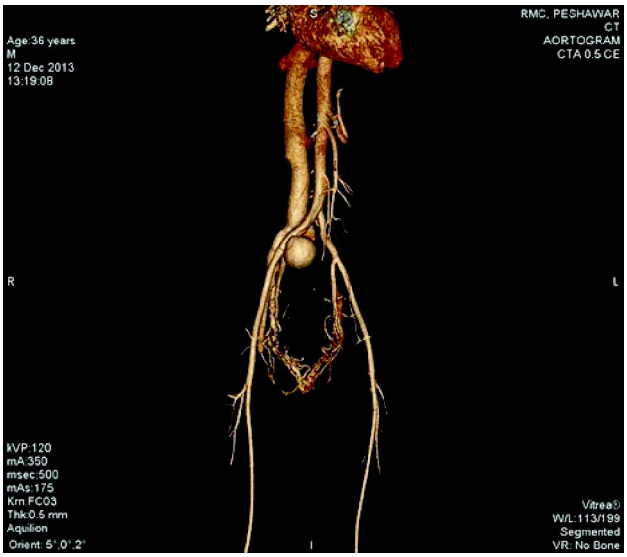

Figure 10: CT Aortogram of a 36 years old male showing AVF of right iliac vessels with aneurysmal dilatation.

Congenital Aortic diseases:

Right aortic arch:

Right aortic arch was seen in 2% cases. It is usually asymptomatic, rare and can be associated with congenital heart diseases. An aberrant left subclavian artery in association with a right-sided aortic arch is the most common type of right-arch anomaly. CTA can visualize the right aortic arch and various branching patterns directly and evaluate the associated heart disease correctly.

Aberrant subclavian artery:

Was seen in 2% cases. 4 cases had kommerell's diverticulum, which is characterized by an ectatic infundibulum at the origin of an anomalous right subclavian artery (Fig. 6) that originates distal to the left subclavian artery in a left-sided arch configuration. The infundibular origin may become aneurysmal and often exhibits circumferential atherosclerotic changes. One of our patients had significant atherosclerotic stenotic disease of aberrant subclavian artery (Fig. 11).

Coarctation:

Coarctation of the aorta is a congenital malformation and typically a disease of childhood and early adulthood.[24] Coarctation of the aorta can occur anywhere along the course of the vessel. Coarctation is most commonly manifested as a focal narrowing or dia-

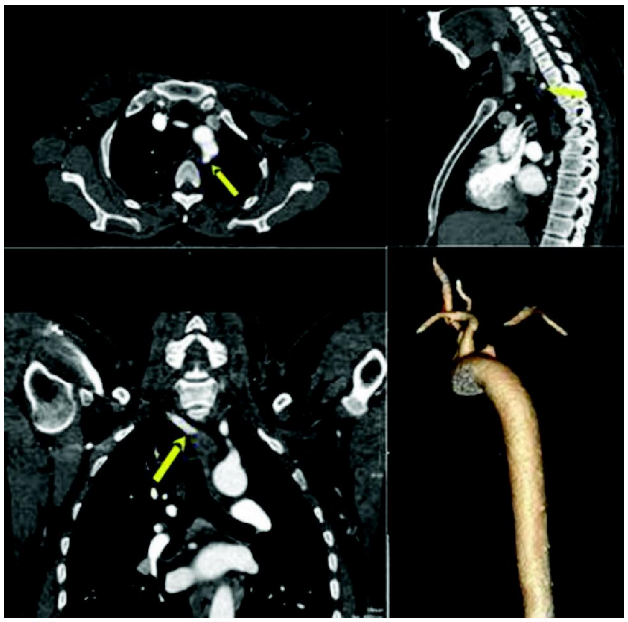

Figure 11: 40 year old female with thrombosed aberrant right subclavian artery

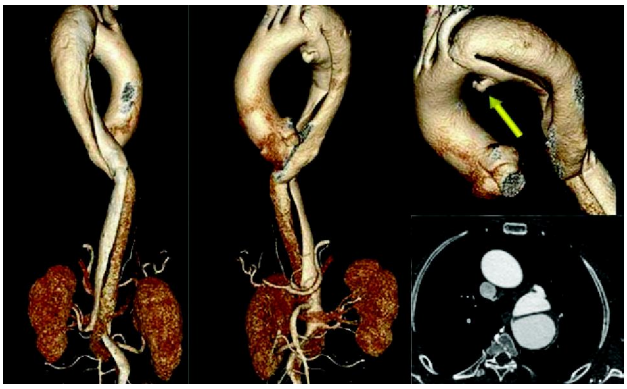

Figure 12: 55-year-old female, post coarctation repair with chest pain and hypotension. Curved multiplanar reconstruction and 3D volume rendering of contrast-enhanced CT show Stanford type B dissection separating smaller anterior true lumen from posterior false lumen of descending aortic aneurysm, dissection flap extending up to bifurcation and involving right common iliac artery; a small aneurysm seen (arrow) at the site of previous coarctation.

phragm like ridge in a juxtaductal location. In addition to discrete narrowing, associated hypoplasia may be present and involve a portion or all of the aortic arch.[25] The diagnosis of coarctation of the aorta can usually be made on clinical grounds but imaging is necessary to evaluate the exact anatomy of the lesion and to detect associated abnormalities. In our study, 20 patients had coarctation of aorta and 2 had complete interrupted aortic arch. Role of CT in patients with aortic coarctation is to detect associated cardiac anomalies, the diameter of the aorta especially after treatment to assess stability of the repair and detect complications early, for depiction and quanti-fication of post stenosis dilatation, ascending aortic ectasia, aortic arch hypoplasia and recoarctation or formation of a local aneurysm or pseudoaneurysm at the previous site of coarctation (Fig. 12).

Midaortic Syndrome:

Middle aortic syndrome (MAS) is a rare entity characterized by localized narrowing of abdominal or distal thoracic aorta.[26] One of our patients had a long narrow segment of abdominal aorta. There was occlusion of celiac trunk and superior mesenteric arteries with resultant opening up of various collateral pathways like arc of Riolan (Fig. 13).

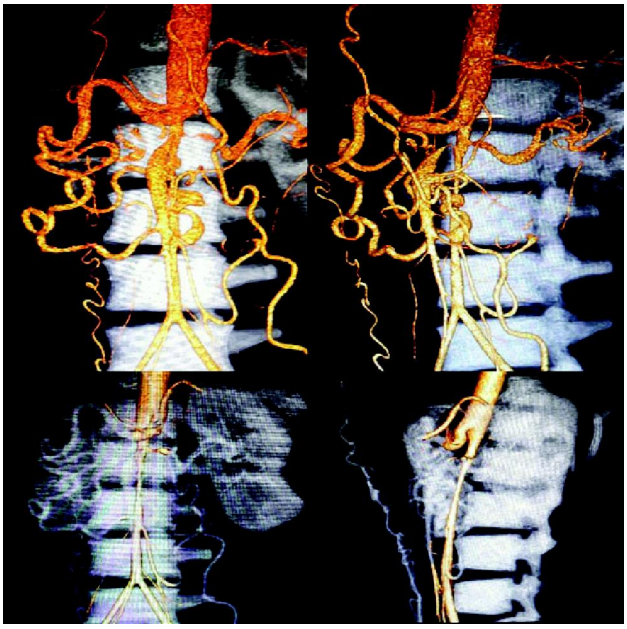

Figure 13: CT Aortogram 3D surface rendered images showing midaortic syndrome.

Coronary artery anomalies:

Coronary anomalies were seen in two of the patients who underwent CT Aortography. One patient had a single coronary artery.

In reports of previous studies that used helical CT for evaluation of aorta, researchers have suggested that multiplanar reconstructions created from helical CT dataset, may add useful information.[27] This was confirmed in our study.

Conclusion

CT is the ideal noninvasive imaging examination for the evaluation of aortic abnormalities. Knowledge of the imaging appearances of aortic lesions enables preoperative or interventional assessment and post-procedural followup for detection of complications.

Acknowledgements:
Special Thanks to Mr. Arshad Ali for his typing skills and technical support in data compilation.

References

1. Kimura-Hayama ET, Meléndez G, Mendizábal AL, Meave-González A, B. Zambrana GF and Corona-Villalobos CP. Uncommon Congenital and Acquired Aortic Diseases: Role of Multidetector CT Angiography. RadioGraphics. 2010; **30(1):** 79-98.

2. Rajiah P. CT and MRI in the Evaluation of Thoracic Aortic Diseases.Int J Vasc Med 2013;**79:** 71-89.

3. Litmanovich D, Bankier AA, Cantin L, Raptopoulos V and Boiselle PM. CT and MRI in Diseases of the Aorta. American Journal of Roentgenology. 2009; **193(4):** 928-40.

4. Bosniak MA. An analysis of some anatomic roentgenologic aspects of the brachio-cephalic vessels. Am J Roentgenol Radium Ther Nucl Med. 1964; **91:** 1222-31.

5. Van De Graaff KM. Human anatomy, 6th ed. New York, NY: McGraw-Hill, 2001; **5:** 74-83.

6. Ucerler H, Ikiz Z AA. Multiplicity of the variations in ventral branches of abdominal aorta. Ital J Anat Embryol. 2006; **111:** 15-22.

7. Mao SS, Ahmadi N, Shah B. Normal thoracic aorta diameter on cardiac computed tomography in healthy asymptomatic adults: impact of age and gender. Acad Radiol 2008; **15:** 827-34 .

8. Aronberg DJ, Glazer HS, Madsen K, Sagel SS. Normal thoracic aortic diameters by computed tomography. J Comput Assist Tomogr.1984; **8:** 247-50.

9. Hager A, Kaemmerer H, Hess J. Comparison of helical CT scanning and MRI in the follow-up of adults with coarctation of the aorta. Chest 2005; **127:** 2296

10. Scott RA, Ashton HA, Kay DN. Abdominal aortic aneurysm in 4,237 screened patients: prevalence, development, and management over 6 years. Br J Surg. 1991; **78:** 1122-5.

11. Hager A, Kaemmerer H, Rapp-Bernhardt U. Diameters of the thoracic aorta throughout life as measured with helical computed tomography. J Thorac Cardiovasc Surg. 2002; **123:** 1060-6.

12. Tops LF, Wood DA, DelgadoV. Non invasive evaluation of the aortic root with multislice computed tomography. JACC: Cardiovascular Imaging. 2008; **1(3):** 321-30.

13. Litmanovich D, Bankier AA, Cantin L, Raptopoulos V and Boiselle PM. CT and MRI in diseases of the aorta. The American Journal of Roentgenology. 2009; **193(4):** 928-40.

14. Burman ED, Keegan J and KilnerPJ. Aortic root measurement by cardiovascular magnetic resonance: specification of planes and lines of measurement and corresponding normal values. Circulation: Cardiovascular Imaging. 2008; **1(2):** 104-13.

15. AgarwalPP, Chughtai A, MatzingerFRK, and Kazerooni EA. Multidetector CT of thoracic aortic aneurysms. Radiographics. 2009; **29(2):** 537-52.

16. Svensson LG, Crawford ES, Hess KR, Coselli JS, and Safi, HJ. Experience with 1509 patients undergoing thoracoabdominal aortic operations. Journal of Vascular Surgery. 1993; **17(2):** 357-68.

17. Castañer E, Andreu M, Gallardo X, MataJM, Cabezuelo MA, and Pallardó Y. CT in nontraumatic

acute thoracic aortic disease: typical and atypical features and complications. Radiographics. 2003; **23:** 93-110.

18. Mahon MA and Squirrell CA. MultidetectorCTof aortic dissection: a pictorial review. Radiographics. 2010; **30(2):** 445-60.

19. Gotway MB, Araoz PA, MacedoTA. Imaging findings in Takayasu's arteritis. The American Journal of Roentgenology. 2005; **184(6):** 1945-50.

20. Desai MY, Stone JH, Foo TKF, Hellmann DB, Lima JAC and Bluemke DA. Delayed contrast-enhanced MRI of the aortic wall in Takayasu's arteritis: initial experience.The American Journal of Roentgenology. 2005; **184(5):** 427-1431.

21. Kuhlman JE, Pozniak MA, Collins J and Knisely BL. Radiographic and CT findings of blunt chest trauma: aortic injuries and looking beyond them. Radiographics.1998; **18(5):** 1085-106.

22. Kronzon I, Tunick PA. Aortic Atherosclerotic Disease and Stroke. Circulation. 2006; **114:** 63-75.

23. HardmanRL, Lopera JE, Cardan RA, Trimmer CK, Josephs SC. Common and Rare Collateral Pathways in Aortoiliac Occlusive Disease: A Pictorial Essay. American Journal of Roentgenology. 2011; **197(3):** 519-24.

24. Al-Azzazya MZ, Nasrb MS, Shourac MA. Multidetector computed tomography (MDCT) angiography of thoracic aortic coarctation in pediatric patients: Pre-operative evaluation. The Egyptian Journal of Radiology and Nuclear Medicine, March 2014; **45(1):** 159-67.

25. Dillman JR, Hernandez RJ. Role of CT in the Evaluation of Congenital Cardiovascular Disease in Children. American Journal of Roentgenology. 2009; **192:** 1219-31.

26. Bhatti AM, Mansoor J, Younis U, Siddique K, ChattaS.Mid aortic syndrome: A rare vascular disorder. J Pak Med Assoc Oct 2011; **61(10):** 1018-20.

27. L E Quint, I R Francis, D M Williams, J C Bass, M J Shea, D L Frayer, H M Monaghan, and G M Deeb. Evaluation of thoracic aortic disease with the use of helical CT and multiplanar reconstructions: comparison with surgical findings. Radiology 1996; **201(1):** 37-41.